RSC Advances

PAPER

View Article Online
View Journal | View Issue

Cite this: *RSC Adv.*, 2014, **4**, 23554

Bent-core luminescent and electroactive bis(triazolyl)triazines with compact columnar mesomorphism†

Eduardo Beltrán,[a] Beatriz Robles-Hernández,[b] Nerea Sebastián,[b] José Luis Serrano,[c] Raquel Giménez*[a] and Teresa Sierra*[a]

Received 2nd April 2014
Accepted 12th May 2014

DOI: 10.1039/c4ra02926g

www.rsc.org/advances

The bulk self-assembly of bent-core molecules based on the novel structure 2-methoxy-4,6-bis(1′,2′,3′-triazol-4′-yl)-1,3,5-triazine is reported together with their luminescent and electrochemical properties. Two families of compounds with lateral branches of different lengths have been investigated. Columnar mesomorphism with short stacking distances and periodic twisted structures were found. A compound exhibiting two hexagonal columnar mesophases that show different emission spectra and a transition from a bimolecular assembly to a unimolecular assembly is described.

Introduction

Columnar liquid crystals have the ability to spontaneously aggregate into stacks and this represents an interesting approach to one-dimensional soft anisotropic systems for the transport of electrons, ions, energy, photons or molecules.[1–4] Properly designed columnar mesogens have demonstrated good performance in optoelectronic devices.[5–11]

Columnar mesophases are mainly based on discotic molecules[12,13] but molecules with different shape anisotropies,[14,15] such as star-shaped molecules,[16] T-shaped molecules,[17] phasmidics,[18,19] dendrimers,[20–23] bowl-shaped,[24–29] half-disk,[30–32] taper-shaped[33–35] or bent-core[36] molecules as examples, can also provide columnar mesophases. A delicate balance between non-covalent interactions such as H-bonding, π-stacking, van der Waals forces, microsegregation and steric effects provides the driving force for the effective filling of the free volume in a columnar arrangement.

The bent-core geometry is, of the unconventional shapes, an example of the tight relationship between molecular structure, supramolecular arrangement and properties of the material. Furthermore, this system highlights the importance of the assembly in transferring the molecular properties to the macroscopic level or in finding new and exciting properties on the micro- or nanoscale. Bent-core liquid crystals are achiral organic molecules that generally contain a 120° disubstituted aromatic ring and they are able to pack in a compact way to form lamellar or columnar phases.[36–38] Some of the mesophases are endowed with chirality or polarity, and excellent properties that include ferroelectric or antiferroelectric behaviour, piezoelectricity, or nonlinear optical properties have been reported.[39–41] The columnar arrangements found with these compounds are different to regular stacks of molecules and are actually defined as modulated phases formed by frustrated layers.[42] On the other hand, the formation of properly stacked molecules in columnar mesophases of bent-core molecules has also been observed in some cases,[43–45] and the interest in these systems lies in the possibility of obtaining a macroscopic polarization along the columnar axis and polar switching.[46–52]

Heterocyclic derivatives have been widely explored in the molecular design of columnar liquid crystals, as the dipole originating from the heteroatoms plays an important role in the columnar stabilization and may give rise to additional properties such as increased electron affinity, as occurs for nitrogen-rich aromatics (azaaromatics).[53] In this regard, we recently described the synthesis and properties of a new class of compounds based on the nitrogen rich star-shaped core 2,4,6-tris(1′,2′,3′-triazol-4′-yl)-1,3,5-triazine, which show columnar mesomorphism, luminescence and electron-acceptor characteristics.[54,55] The triazole rings joined to the triazine ring confer flexibility to the core and this enabled these molecules to adopt unusual assemblies with different symmetry conformations in the columns.[55]

The aim of the work described here was to study the properties of the triazine–triazole group in a bent-core structure, based on the special self-assembly that this geometry provides. Thus, the synthesis and characterisation of novel compounds derived from 2-methoxy-4,6-bis(1′,2′,3′-triazol-4′-yl)-1,3,5-triazine and their bulk self-assembly in mesomorphic columnar structures are reported.

---

[a] *Departamento de Química Orgánica, Instituto de Ciencia de Materiales de Aragón (ICMA) – Facultad de Ciencias, CSIC – Universidad de Zaragoza, 50009 Zaragoza, Spain. E-mail: rgimenez@unizar.es; tsierra@unizar.es; Tel: +34 976 762276*

[b] *Departamento de Física Aplicada II, Facultad de Ciencia y Tecnología, Universidad del País Vasco UPV/EHU, 48080 Bilbao, Spain*

[c] *Instituto de Nanociencia de Aragón (INA), Edificio I+D, Universidad de Zaragoza, 50018 Zaragoza, Spain*

† Electronic supplementary information (ESI) available: Synthetic procedures and characterisation data, DSC thermograms, UV-Vis and emission spectra and electrochemical data. See DOI: 10.1039/c4ra02926g

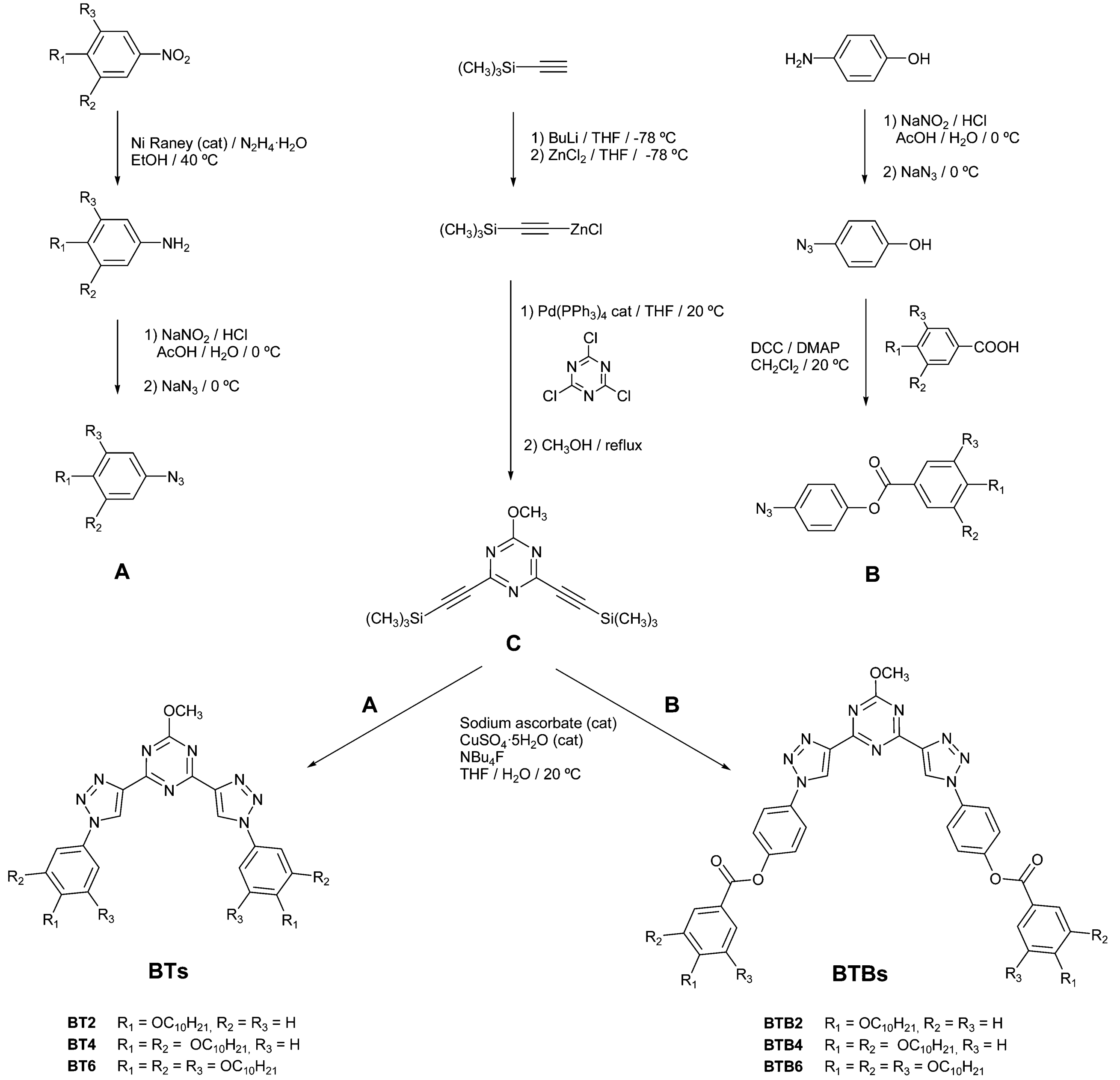

Scheme 1 Synthetic pathway followed for the preparation of **BTs** and **BTBs**.

The stacking found along the columns is compact with short intermolecular distances. The molecules are fluorescent and electroactive, thus endowing the assemblies with these properties. Two families of compounds (**BTs** and **BTBs**) with lateral branches of different lengths have been investigated (Scheme 1).

Results and discussion

Synthesis

The synthetic route followed is depicted in Scheme 1. In order to obtain the compounds with the bent shape, the core 2-methoxy-4,6-bis(trimethylsilyl)-1,3,5-triazine, **C**, was synthesised by reaction of two moles of chlorotrimethylsilylethynylzinc(II) per mol of cyanuric chloride by a Negishi coupling.[56,57] In a second synthetic step, an excess of methanol was added and the reaction mixture was heated under reflux in order to introduce the methoxy group into the triazine ring, thus affording **C** in 57% yield. According to the expected molecular structure, the ^{1}H-NMR spectrum shows two singlets, which correspond to the methoxy group (4.07 ppm) and the trimethylsilyl group (0.28 ppm).

The target **BTs** and **BTBs** were prepared by direct reaction of **C** with the aromatic azides **A** or **B** by adapting a synthetic procedure previously described for tris(triazolyl)triazines.[54] The reaction gave the products in 60–80% yield at room temperature and in one-pot. The process involves two orthogonal reactions, the double alkyne deprotection and the double 1,3-dipolar cycloaddition of the aromatic azides to the alkyne groups catalyzed by copper(I) (CuAAC click reaction[58]).

The ^{1}H-NMR spectra display a singlet corresponding to the C5 proton of the triazolyl ring at 8.9–9.0 ppm, indicating that the 1,4-disubstituted triazole regioisomer is formed. In addition, both series show a singlet corresponding to the methoxy group at 4.30 ppm. The results indicate the compatibility of this methodology with the methoxy substitution of the triazine ring.

Liquid crystalline behaviour and self-assembly models

The thermal properties and the liquid crystalline behaviour of **BTs** and **BTBs** were investigated by thermogravimetric analysis (TGA), polarising optical microscopy (POM), differential scanning calorimetry (DSC) and X-ray diffraction (XRD). The transition temperatures and enthalpy values are collected in Table 1. The mesophase parameters obtained by XRD are summarised in Table 2. Compounds of the **BT** series with four and six terminal chains, **BT4** and **BT6**, and the compound of the **BTB** series with six terminal chains, **BTB6**, are columnar liquid crystals. The other compounds are crystalline solids that melt directly to the isotropic liquid. For **BTB2** a decomposition process takes place along with the transition to the isotropic liquid and, prior to this, an unknown phase with a lamellar arrangement was observed in some experiments. However, the lack of reproducibility between DSC cycles (ESI, Fig. S1†) did not allow us to draw firm conclusions.

Compound **BT4** displayed a columnar phase from room temperature up to 104 °C, at which point the transition to the isotropic liquid occurred. In the cooling process, two transitions were observed due to the appearance of an additional columnar mesophase over a small temperature range (monotropic mesophase). The DSC thermogram shows that the two transitions are partially overlapped (ESI, Fig. S2†). By POM, a pseudofocal-conic texture of a columnar mesophase started to appear at 100 °C on cooling the isotropic liquid (Fig. 1a, inset) and a decrease in birefringence was observed on further cooling at 94 °C (Fig. 1a). The XRD pattern obtained at room temperature for compound **BT4** shows three reflections in the small angle region in a ratio $1:1/\sqrt{3}:1/\sqrt{7}$, which is consistent with a hexagonal symmetry for the columnar mesophase (Fig. 2a). In the high angle region, the typical diffuse halo at 4.4 Å, related to the fluid character of the decyloxy tails, and two additional reflections located at 3.8 Å and 3.4 Å, which are related to stacking, are observed. These latter two reflections are indicative of a certain 3D order of the phase and are compatible with a hexagonal plastic columnar phase[13] (Col$_{\text{hp}}$) with a cell parameter of 33.7 Å. A diffractogram of the monotropic mesophase of **BT4** was obtained by rapid cooling at room temperature and this shows only a sharp maximum in the small angle region and a diffuse halo at 4.3 Å (Fig. 2b). This kind of pattern does not unambiguously confirm a hexagonal symmetry but rules out other columnar symmetries and it has been observed for hexagonal columnar phases of several non-conventional mesogens.[43,59–63] The diffractogram, together with the observed POM texture, led us to propose that the small-angle maximum corresponds to the (10) reflection of a hexagonal columnar mesophase with a cell parameter (a) of 35.6 Å. Taking into account the cell parameter of these two columnar phases, the unit cell should contain about two molecules ($Z = 2$) on the reasonable assumption that the density is around 1 g cm^{-3}.[64] On the basis of these data, a model is proposed for the molecular arrangement in a columnar stratum in which two bent-core molecules are disposed with their molecular dipoles in an antiparallel manner to form a disk like unit (Fig. 2c). This arrangement allows efficient space filling and a partial interdigitation of the polar methoxytriazine groups belonging to two antiparallel molecules.

Table 1 Phase behaviour[a] of BTs and BTBs

Compound	T/°C (ΔH/kJ mol^{-1})[b]
BT2	Cr 13 (3.8) [Cr′ + Cr″] 169[c] (37.6) I
	I 164 (22.4) Cr″ 141 (9.0) Cr′ 12 (4.1) Cr
BT4	Col$_{\text{hp}}$ 104 (29.9) I
	I 100 Col$_{\text{h}}$ 96 (27.5) Col$_{\text{hp}}$
BT6	Col$_{\text{h}}^{\text{A}}$ 59 (13.2) Col$_{\text{h}}^{\text{B}}$ 121[c] (7.6) I
	I 116 (9.2) Col$_{\text{h}}^{\text{B}}$ 42 (13.0) Col$_{\text{h}}^{\text{A}}$
BTB2	Cr 85 (12.9) P 243 I + Dec
BTB4	Cr 115 (37.8) Cr′ 194 (48.4) I
	I 189 (47.3) Cr′ 86 (51.2) Cr
BTB6	Col$_{\text{h}}$ 172 (27.5) I
	I 166 (29.4) Col$_{\text{h}}$

[a] Col$_{\text{h}}$ = hexagonal columnar mesophase, Col$_{\text{hp}}$ = hexagonal plastic columnar phase, Cr = crystalline phase, I = isotropic liquid, Dec = decomposition process, P = unknown phase. [b] Onset temperatures from DSC heating and cooling cycle at 10 °C min^{-1}. [c] Temperature corresponding to the maximum of a broad peak.

Table 2 XRD data for the liquid crystalline phases

Compound	T/°C	Phase	d/Å	hk	Parameters[a]
BT4	20	Col$_{\text{hp}}$	29.6	10	$a = 33.7$ Å
			16.8	11	
			10.9	21	
			4.4 (br)		
			3.8		
			3.4		
	20[b]	Col$_{\text{h}}$	30.8		$a = 35.6$ Å
			4.4 (br)		
BT6	20	Col$_{\text{h}}^{\text{A}}$	31.8	10	$a = 36.9$ Å
			18.6	11	$c = 3.3$ Å
			15.5[c]		
			4.3 (br)		
			3.3[c]	01	
	100	Col$_{\text{h}}^{\text{B}}$	26.0	10	$a = 30.0$ Å
			12.7[c]		
			4.5 (br)		
BTB6	20	Col$_{\text{h}}$	37.4	10	$a = 43.2$ Å
			15.1[c]		$c = 3.4$ Å
			4.4 (br)		
			3.4[c]	01	

[a] $a = (2/\sqrt{3})\ ((d_{10}) + (d_{11})\sqrt{3} + (d_{20})\sqrt{4} + (d_{21})\sqrt{7} + \ldots/n_{\text{reflections}})$. [b] Sample heated at 100 °C and rapidly cooled down to 20 °C. [c] Reinforced along the meridian in an oriented pattern. (br) = broad halo.

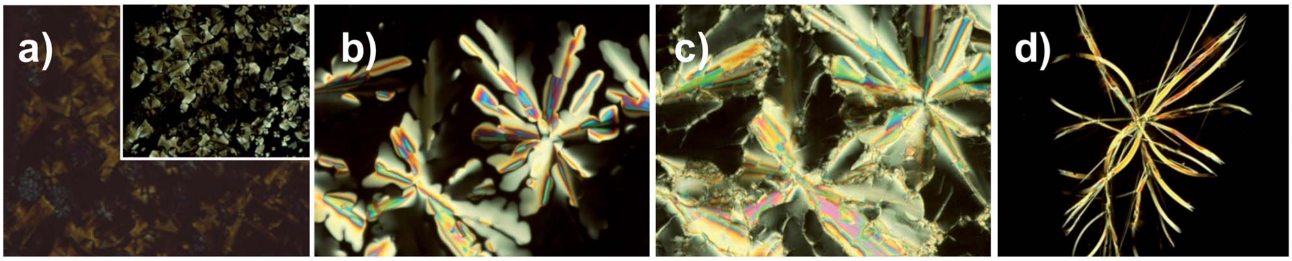

Fig. 1 Textures observed by POM in the cooling process between crossed polarisers (a) **BT4** in the Col$_{hp}$, (94 °C), inset corresponds to the Col$_h$ (100 °C), (b) **BT6** in the Col$_h^B$ (112 °C), (c) **BT6** in the Col$_h^A$ (20 °C) and (d) **BTB6** in the Col$_h$ (161 °C).

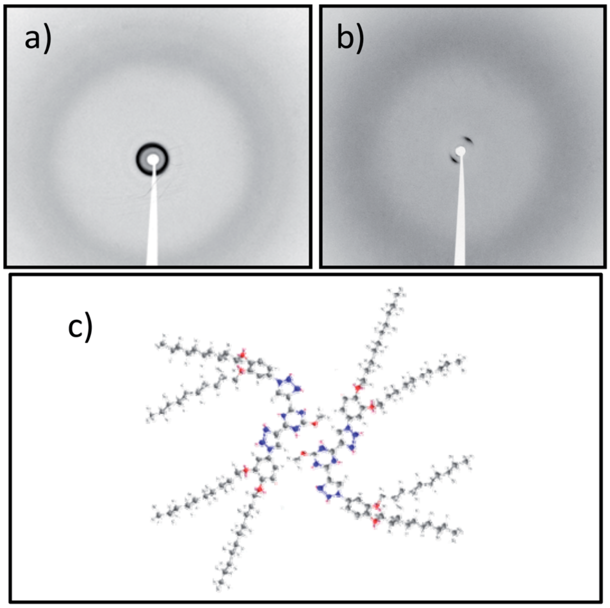

Fig. 2 Diffractograms corresponding to **BT4** in (a) Col$_{hp}$ and (b) Col$_h$. (c) Proposed model for the arrangement of two molecules of **BT4** in a columnar slice.

Compound **BT6** displays two enantiotropic hexagonal columnar mesophases (ESI, Fig. S3†). In the cooling process, a dendritic texture typical of a columnar mesophase developed at 116 °C (Fig. 1b). This texture became blurred at 42 °C, *i.e.*, at the transition to another columnar mesophase, and remained stable at room temperature (Fig. 1c). The diffractogram observed for the room temperature mesophase (Col$_h^A$) is consistent with a hexagonal columnar mesophase with a cell parameter (a) of 36.9 Å and intracolumnar order with a stacking periodicity (c) of 3.3 Å (Fig. 3a). For the high temperature mesophase (Col$_h^B$) a cell parameter of 30.0 Å, which is much smaller than the low temperature phase, was measured and there is a loss of the regular molecular stacking along the columns (Fig. 3b and Table 2). Based on density calculations for the unit cell similar to those performed for **BT4**, the low temperature mesophase should contain about two molecules per unit cell (Z = 2), whereas the high temperature mesophase, with a 6.9 Å decrease in the (a) parameter, should contain only one (Z = 1). This means that in the Col$_h^A$-to-Col$_h^B$ transition there is a change in the mode of arrangement, from a bimolecular assembly to a unimolecular assembly. A similar decrease in the cell parameter has been reported for derivatives of tris(triazolyl)triazine when they show bimolecular or unimolecular arrangements in the columnar mesophase.[8] It is remarkable that in this case, the triazine–triazole group is in a different molecular geometry, a bent-shape and not a star-shape, and the two different columnar arrangements with hexagonal symmetry are found in the same compound with a first-order transition between them.

For both mesophases, it was also possible to prepare partially aligned samples (Fig. 3c and d). It was observed that some maxima were reinforced in the meridian region (direction parallel to the columnar axis), indicating that there are additional periodic modulations of the electronic density along the columns. In the room temperature mesophase (Col$_h^A$) these maxima are found at 15.5 Å and 3.3 Å. To account for this we propose a model in which two molecules are arranged in an antiparallel manner in a column slice (Fig. 4a), and these dimers are stacked at 3.3 Å and arranged periodically along the columnar axis, in such a way that each slice is rotated along the column in order to give a periodicity of 15.5 Å. This situation can be explained by considering that there is a repetitive situation every 15.5/3.3 slices, *i.e.*, approximately 4.5 dimers. Since

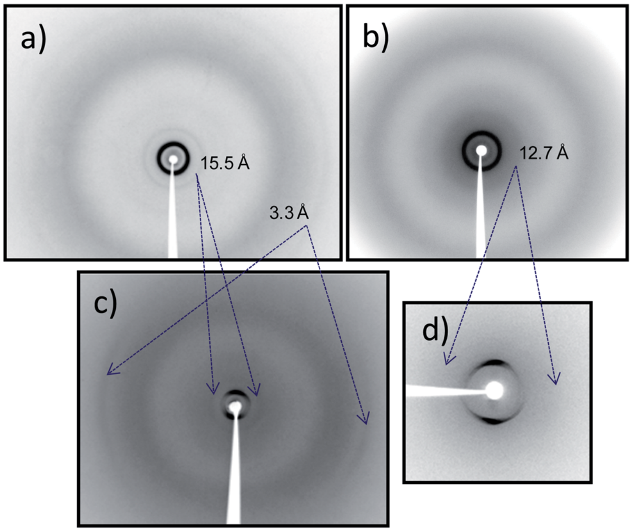

Fig. 3 Diffractograms corresponding to compound **BT6** in (a) Col$_h^A$ at 20 °C and (b) Col$_h^B$ at 100 °C, (c) partially oriented pattern at 20 °C, (d) partially oriented pattern at 100 °C.

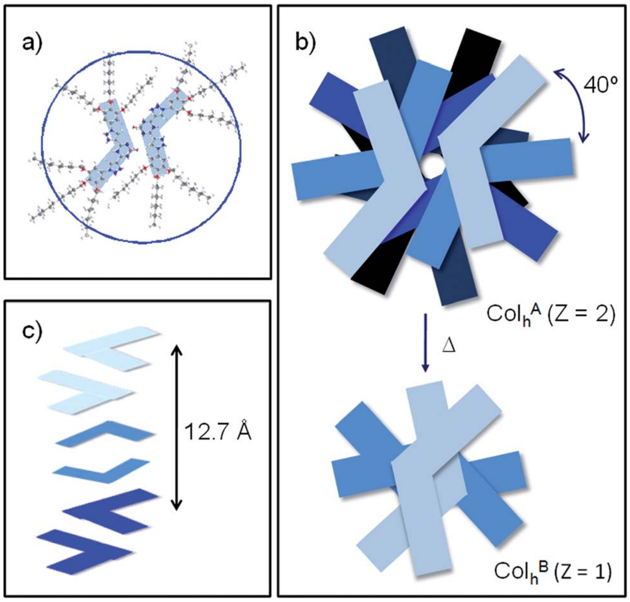

Fig. 4 (a) Proposed model for the arrangement of two molecules of **BT6** in the Col$_\text{h}^\text{A}$ mesophase. (b) Top view of the arrangement in the Col$_\text{h}^\text{A}$ and (b) Col$_\text{h}^\text{B}$ mesophases. Columnar stacking is represented by different colours. (c) Side view of the Col$_\text{h}^\text{B}$.

each dimer has a binary symmetry axis, 4.5 dimers or 9 molecules mutually rotated by 40° will constitute a 180° turn (Fig. 4b). Therefore, in a 360° full turn there will be 9 dimers (18 molecules) and the twisted periodic structure will have a pitch distance of $15.5 \times 2 = 31$ Å.

In the case of the high temperature mesophase (Col$_\text{h}^\text{B}$), with $Z = 1$, the interdisk distance is not observed but there is a diffuse maximum that is reinforced in the meridian at a distance of 12.7 Å. This can be assigned to a stacking correlation of about 4 molecules, for which we propose an arrangement of the four molecules as two interdigitated dimers mutually rotated by 90° (Fig. 4c). Thus, the transition Col$_\text{h}^\text{A}$-to-Col$_\text{h}^\text{B}$ on heating can be visualised as follows, the two molecules of the dimer situated in one columnar slice in the low temperature phase start to interdigitate and overlap, resulting in stacking of interdigitated antiparallel dimers (Fig. 4b), thus leading to a decrease in the diameter of the columns.

In view of these arrangements and the possible orientation of the polar molecules along a column to give rise to a polar response, electric fields up to 60 V μm^{-1} were applied by sandwiching **BT6** in a Linkam cell (5 μm thick). The sample was very viscous and reorientation effects or polar switching was not observed in either of the two mesophases. The dielectric permittivity at 1 kHz was measured using an HP4192 impedance analyzer. The transition between the two columnar phases, as well as the transition to the isotropic phase, was clearly visible as a change in the dielectric permittivity (Fig. 5). However, despite the fact that both columnar phases have a rather low permittivity value, this value is lower in the high temperature Col$_\text{h}^\text{B}$ and this could be due to the interdigitated antiparallel arrangement of the dimers.

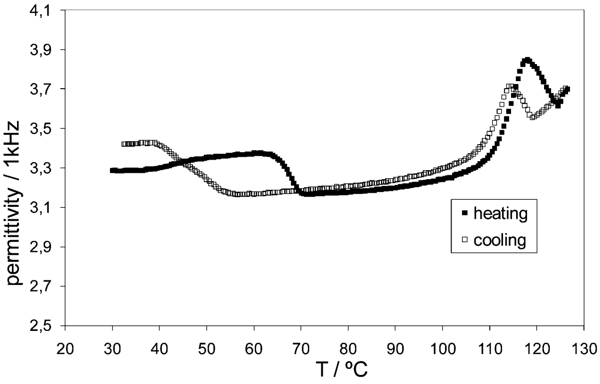

Fig. 5 Change in the dielectric permittivity of **BT6** on cooling and heating at 1 °C min^{-1}.

Compound **BTB6** exhibits a stable enantiotropic columnar mesophase from room temperature up to the clearing point at 172 °C. Curled birefringent filaments were observed by POM on cooling from the isotropic liquid into the mesophase (Fig. 1d). The enthalpy value, 29.4 kJ mol^{-1}, is consistent with a highly ordered mesophase and the fluidity found at room temperature demonstrates the mesomorphic nature (ESI, Fig. S4 and S5†). The XRD pattern only displays a reflection in the low angle region but, together with two additional reflections that are reinforced in an orthogonal direction, this allows us to assign the mesophase as hexagonal columnar with a cell parameter of 43.2 Å and a periodic interdisk distance of 3.4 Å. Density estimations indicate that the number of molecules per unit cell is two ($Z = 2$). Analysis of a partially aligned sample of this compound revealed that, as before, there are two reflections that are reinforced in the meridian region, one at 3.4 Å (interdisk distance) and an additional one at 15.1 Å (Fig. 6). In contrast to **BT6** the reflections are unusually strong and are very well defined, which indicates that the intracolumnar order has a longer range.[62] These results are also in agreement with the type of growth of the mesophase texture from the isotropic liquid. As discussed for the Col$_\text{h}^\text{A}$ phase of **BT6**, the intramolecular periodic distance of 15.1 Å led us to propose a similar arrangement for **BTB6**, in which there is a twisted periodic structure formed by

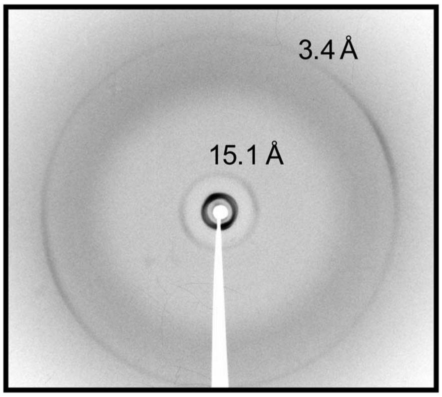

Fig. 6 Partially oriented pattern for **BTB6** at 20 °C.

Table 3 UV-Vis absorption and emission data for **BTs** and **BTBs**

Compound	λ_{abs}^{THF}/nm (log ε)	$\lambda_{abs}^{cyclohexane}$/nm (log ε)	λ_{em}^{THF}/nm	$\lambda_{em}^{cyclohexane}$/nm	λ_{abs}^{film}/nm	λ_{em}^{film}/nm	Φ
BT2	283 (4.63), 289^{sh} (4.61)	—[a]	366	—[a]	270, 286^{sh}	405	0.10[b]
BT4	277 (4.73)	283 (3.67), 300 (3.50)	446	380	254, 302	459	0.64[b]
BT6	255 (4.50), 294 (4.61)	253 (4.49), 293 (4.50)	464	397	266, 305	473	0.13[b]
BTB2	275 (4.97)	—[a]	378	—[a]	282	441	≤0.01[c]
BTB4	273 (4.92), 291 (4.85)	276 (3.84), 295 (3.81)	376	393	273, 295, 303^{sh}	425	≤0.01[c]
BTB6	284 (4.87)	283 (4.93)	375	347	284	406	≤0.01[c]

[a] Low solubility. [b] Quantum yields in THF relative to 9,10-diphenylanthracene ($\Phi = 0.9$ in cyclohexane).[69] [c] Quantum yields in THF relative to 2-(4-biphenylyl)-5-phenyl-1,3,4-oxadiazole (PBD) ($\Phi = 0.8$ in benzene).[70]

4.5 stacked dimers (9 molecules) mutually rotated by 40° along the columnar axis. Therefore, for **BTB6** a similar model to the one represented for the Col_h^A of **BT6** would apply (Fig. 4b).

Absorption and emission properties

UV-Vis and fluorescence spectra were recorded on dilute solutions in tetrahydrofuran (THF) or cyclohexane and in thin films at room temperature (Table 3).

In solution, for both **BTs** and **BTBs** the maximum absorption is located in the UV spectrum below 300 nm and, due to their absorption coefficient values, is consistent with π–π* transitions. In the condensed phase the profile is similar to that obtained for the solutions but with small red-shifts. Compounds of the **BT** series are fluorescent in THF solution in the blue-green region of the visible spectrum and they have low or moderate quantum yield values. The emission maxima are dependent on the number of peripheral long tails, with a clear red-shift observed when the number increases from two to six. The Stokes shifts therefore increase, with values of 82 nm, 169 nm and 170 nm for **BT2**, **BT4** and **BT6**, respectively. These values are consistent with a higher charge transfer and/or conformational relaxation in the excited state on increasing the number of peripheral chains, as described for star-shaped compounds with a similar triazole–triazine group[54] or with other nitrogenated mesogens.[63,65] The emission maxima are also red-shifted on increasing the polarity of the solvent from cyclohexane to THF. This effect is found in molecular systems with electron donor groups (alkoxy) linked to an electron acceptor group (triazine) by a similar conjugated system[55] and it is known as positive solvatofluorochromism.[66]

For the **BTB** series the emission bands in solution appear in the near-UV region, the emission maxima in THF are almost insensitive to the number of long tails of the compounds and the Stokes shift values are around 100 nm. The main difference between **BTs** and **BTBs** is that the introduction of the benzoyloxy groups increased the possibility of non-radiative deactivation pathways and much lower quantum yield values than for **BT** series are found.

All compounds show luminescence as thin films at room temperature in the blue-green region of the visible spectrum. **BT** derivatives show, as in solution, a red-shift on increasing the number of chains at the periphery. The opposite is found for the **BTBs**, indicating that in this case the polarity of the excited states is different. The emission spectra of **BT6** in both columnar phases were also measured (Fig. 7). The spectra of the two phases show a broad band consistent with compact or homogeneous packing, but at slightly different wavelengths, 473 nm for Col_h^A and 464 nm for Col_h^B. The longer emission wavelength of the low temperature mesophase is consistent with the observed longer degree of intracolumnar order.[67]

Electrochemical properties

The electrochemical properties of the compounds were studied by cyclic voltammetry (CV) using a glassy carbon working electrode, a Pt counter electrode, and an Ag/AgCl reference electrode in a three-electrode cell. The experiments were carried out under argon in CH_2Cl_2, with Bu_4NPF_6 as a supporting electrolyte (0.1 M) at a scan rate of 100 mV s^{-1} (ESI, Table S1†). None of the compounds, except for **BT6**, showed any oxidation process between 0 V and +2.2 V. In general, compounds of the **BT** series show two reduction waves located at −1.78 V and −0.92 V (*vs.* Ag/AgCl), for which a LUMO value of −3.40 eV can be calculated. In addition, **BT6** shows an oxidation wave at +1.49 V (*vs.* Ag/AgCl) and this could be due to the higher number of donor chains that make the oxidation of the methoxy group more favourable. For the **BTB** series there is only a reduction wave located at −1.79 eV and this corresponds to a LUMO value of −2.53 eV. Comparison of the LUMO values (−3.40 eV for **BTs** and −2.53 eV for **BTBs**) with the value of a reference compound such as 2,4,6-triphenyl-1,3,5-triazine (−2.71 eV)[68] shows that, as

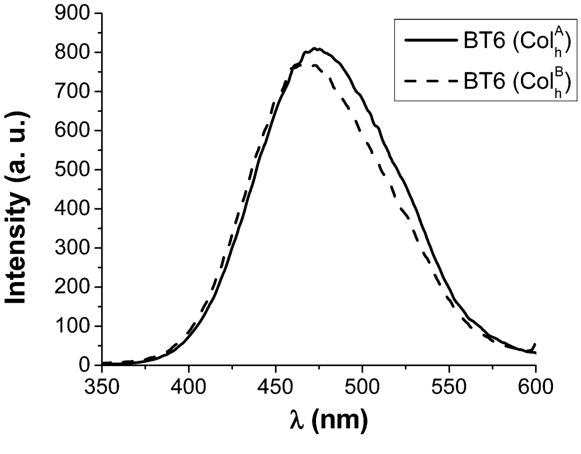

Fig. 7 Emission spectra for **BT6** in a thin film.

observed in the **BT** series, the triazole rings together with the alkoxyphenyl peripheral groups lead to an increase in the electron affinity. When the peripheral groups are alkoxybenzoyloxyphenyl groups, *i.e.*, **BTBs**, the electron affinity decreases in all cases with respect to the parent 2,4,6-triphenyl-1,3,5-triazine, showing a similar behaviour to that of alkoxybenzoyloxyphenyl substituted tris(triazolyl)triazines.[55]

Conclusions

Self-assembled structures with a novel luminescent and electroactive bent-core have been synthesised. The bent-core forces the molecules to be arranged with their molecular dipoles in an antiparallel manner, a situation that leads to hexagonal columnar mesophases over broad temperature ranges. It is remarkable how strongly these molecules tend to self-assemble into regular stacks despite their non-discoid shape. Compounds with six terminal chains exhibit compact stacking with intracolumnar order, and arrangements in a periodic twisted mode. In the particular case of **BT6**, two hexagonal columnar mesophases with a different number of molecules per columnar slice has been found. This different thermally dependent mode of arrangement for the molecules of **BT6** gives rise to different emission spectra. Moreover, LUMO values for the **BT** series are appropriate for electron transport.

Acknowledgements

The authors thank the Gobierno de Aragón and European Union, Fondo Social Europeo (FSE) (research group E04), and the Spanish Ministerio de Economia y Competitividad (MINECO) and European Union, Fondo Europeo para el Desarrollo Regional (FEDER) (Project numbers MAT2012-38538-CO3-01, MAT2012-38538-CO3-02 and CTQ2012-35692), and the Gobierno Vasco (IT-449-10) for financial support. Thanks are given to: Nuclear Magnetic Resonance, Mass Spectrometry, Elemental Analysis and Thermal Analysis Services of the CEQMA, Universidad de Zaragoza-CSIC (Spain).

Notes and references

1. S. Laschat, A. Baro, N. Steinke, F. Giesselmann, C. Hagele, G. Scalia, R. Judele, E. Kapatsina, S. Sauer, A. Schreivogel and M. Tosoni, *Angew. Chem., Int. Ed.*, 2007, **46**, 4832–4887.
2. S. Sergeyev, W. Pisula and Y. H. Geerts, *Chem. Soc. Rev.*, 2007, **36**, 1902–1929.
3. T. Kato, T. Yasuda, Y. Kamikawa and M. Yoshio, *Chem. Commun.*, 2009, 729–739.
4. B. R. Kaafarani, *Chem. Mater.*, 2011, **23**, 378–396.
5. M. O'Neill and S. M. Kelly, *Adv. Mater.*, 2011, **23**, 566–584.
6. L. Schmidt-Mende, A. Fechtenkotter, K. Müllen, E. Moons, R. H. Friend and J. D. MacKenzie, *Science*, 2001, **293**, 1119–1122.
7. V. Percec, M. Glodde, T. K. Beta, Y. Miura, I. Shiyanovskaya, K. D. Singer, V. S. K. Balagurusamy, P. A. Heiney, I. Schnell, A. Rapp, H. W. Spiess, S. D. Hudson and H. Duan, *Nature*, 2002, **419**, 384–387.
8. M. Mathew and Q. Li, in *Self-organized Organic Semiconductors. From Materials to Device Applications*, ed. Q. Li, Wiley, 2011.
9. E. K. Fleischmann and R. Zentel, *Angew. Chem., Int. Ed.*, 2013, **52**, 8810–8827.
10. W. Pisula, M. Zorn, J. Y. Chang, K. Müllen and R. Zentel, *Macromol. Rapid Commun.*, 2009, **30**, 1179–1202.
11. R. J. Bushby and K. Kawata, *Liq. Cryst.*, 2011, **38**, 1415–1426.
12. S. Kumar, *Chem. Soc. Rev.*, 2006, **35**, 83–109.
13. *Chemistry of Discotic Liquid Crystals*, ed. S. Kumar, CRC Press, Boca Raton, 2011.
14. C. Tschierske, *Angew. Chem., Int. Ed.*, 2013, **52**, 8828–8878.
15. C. Tschierske, *Curr. Opin. Colloid Interface Sci.*, 2002, **7**, 69–80.
16. M. Lehmann, in *Top. Curr. Chem. Liquid Crystals – Materials Design and Self-assembly*, ed. C. Tschierske, Springer, Berlin Heidelberg, 2012, vol. 318, pp. 193–224.
17. C. Tschierske, *Chem. Soc. Rev.*, 2007, **36**, 1930–1970.
18. M. Gharbia, A. Gharbi, H. T. Nguyen and J. Malthête, *Curr. Opin. Colloid Interface Sci.*, 2002, **7**, 312–325.
19. H. T. Nguyen, C. Destrade and J. Malthête, *Adv. Mater.*, 1997, **9**, 375–388.
20. B. Donnio, S. Buathong, I. Bury and D. Guillon, *Chem. Soc. Rev.*, 2007, **36**, 1495–1513.
21. B. M. Rosen, C. J. Wilson, D. A. Wilson, M. Peterca, M. R. Imam and V. Percec, *Chem. Rev.*, 2009, **109**, 6275–6540.
22. D. Guillon and R. Deschenaux, *Curr. Opin. Solid State Mater. Sci.*, 2002, **6**, 515–525.
23. M. Marcos, A. Omenat and J. L. Serrano, *C. R. Chim.*, 2003, **6**, 947–957.
24. M. Sawamura, K. Kawai, Y. Matsuo, K. Kanie, T. Kato and E. Nakamura, *Nature*, 2002, **419**, 702–705.
25. G. Cometti, E. Dalcanale, A. Du Vosel and A. Levelut, *Chem. Commun.*, 1990, 163–165.
26. L. Wang, Z. Sun, X. Pei and Y. Zhu, *Chem. Phys.*, 1990, **142**, 335–343.
27. T. M. Swager and B. Xu, *J. Inclusion Phenom. Mol. Recognit. Chem.*, 1994, **19**, 389–398.
28. H. Budig, S. Diele, P. Göring, R. Paschke, C. Sauer and C. Tschierske, *Perkin Trans.*, 1995, 767–775.
29. H. Zimmermann, R. Poupko, Z. Luz and J. Billard, *Z. Naturforsch., A: Phys. Sci.*, 1985, **40**, 149–160.
30. J. Barberá, C. Cativiela, J. L. Serrano and M. M. Zurbano, *Adv. Mater.*, 1991, **3**, 602–605.
31. A. Omenat, J. Barberá, J. L. Serrano, S. Houbrechts and A. Persoons, *Adv. Mater.*, 1999, **11**, 1292–1295.
32. K. Kishikawa, S. Furusawa, T. Yamaki, S. Kohmoto, M. Yamamoto and K. Yamaguchi, *J. Am. Chem. Soc.*, 2002, **124**, 1597–1605.
33. A. G. Serrette and T. M. Swager, *Angew. Chem., Int. Ed.*, 1994, **33**, 2342–2345.
34. G. Ungar, V. Percec, M. N. Holerca, G. Johansson and J. A. Heck, *Chem.–Eur. J.*, 2000, **6**, 1258–1266.
35. S. Moyano, J. Barberá, B. E. Diosdado, J. L. Serrano, A. Elduque and R. Giménez, *J. Mater. Chem. C*, 2013, **1**, 3119–3128.

36 R. A. Reddy and C. Tschierske, *J. Mater. Chem.*, 2006, **16**, 907–961.

37 J. Etxebarria and M. B. Ros, *J. Mater. Chem.*, 2008, **18**, 2919–2926.

38 H. Takezoe and Y. Takanishi, *Jpn. J. Appl. Phys.*, 2006, **45**, 597–625.

39 A. Jákli, I. C. Pintre, J. L. Serrano, M. B. Ros and M. R. De La Fuente, *Adv. Mater.*, 2009, **21**, 3784–3788.

40 I. C. Pintre, J. L. Serrano, M. B. Ros, J. Martínez-Perdiguero, I. Alonso, J. Ortega, C. L. Folcia, J. Etxebarria, R. Alicante and B. Villacampa, *J. Mater. Chem.*, 2010, **20**, 2965–2971.

41 A. Eremin and A. Jákli, *Soft Matter*, 2013, **9**, 615–637.

42 N. Vaupotič, D. Pociecha and E. Gorecka, in *Top. Curr. Chem. Liquid Crystals – Materials Design and Self-assembly*, ed. C. Tschierske, Springer, Berlin, Heidelberg, 2012, vol. 318, pp. 281–302.

43 E. Gorecka, D. Pociecha, J. Mieczkowski, J. Matraszek, D. Guillon and B. Donnio, *J. Am. Chem. Soc.*, 2004, **126**, 15946–15947.

44 E. Gorecka, D. Pociecha, J. Matraszek, J. Mieczkowski, Y. Shimbo, Y. Takanishi and H. Takezoe, *Phys. Rev. E: Stat., Nonlinear, Soft Matter Phys.*, 2006, **73**, 031704.

45 J. Matraszek, J. Mieczkowski, D. Pociecha, E. Gorecka, B. Donnio and D. Guillon, *Chem.–Eur. J.*, 2007, **13**, 3377–3385.

46 H. Takezoe, K. Kishikawa and E. Gorecka, *J. Mater. Chem.*, 2006, **16**, 2412–2416.

47 D. Miyajima, F. Araoka, H. Takezoe, J. Kim, K. Kato, M. Takata and T. Aida, *J. Am. Chem. Soc.*, 2010, **132**, 8530–8531.

48 D. Miyajima, F. Araoka, H. Takezoe, J. Kim, K. Kato, M. Takata and T. Aida, *Science*, 2012, **336**, 209–213.

49 F. Araoka and H. Takezoe, *Jpn. J. Appl. Phys.*, 2014, **53**, 01AA01.

50 D. Miyajima, K. Tashiro, F. Araoka, H. Takezoe, J. Kim, K. Kato, M. Takata and T. Aida, *J. Am. Chem. Soc.*, 2009, **131**, 44–45.

51 C. F. C. Fitie, W. S. C. Roelofs, M. Kemerink and R. P. Sijbesma, *J. Am. Chem. Soc.*, 2010, **132**, 6892–6893.

52 K. Sato, Y. Itoh and T. Aida, *J. Am. Chem. Soc.*, 2011, **133**, 13767–13769.

53 B. Roy, N. De and K. C. Majumdar, *Chem.–Eur. J.*, 2012, **18**, 14560–14588.

54 E. Beltrán, J. L. Serrano, T. Sierra and R. Giménez, *Org. Lett.*, 2010, **7**, 1404–1407.

55 E. Beltrán, J. L. Serrano, T. Sierra and R. Giménez, *J. Mater. Chem.*, 2012, **22**, 7797–7805.

56 A. O. King, E. I. Negishi, F. J. Villani Jr and A. Silveira Jr, *J. Org. Chem.*, 1978, **43**, 358–360.

57 E. I. Negishi and L. Anastasia, *Chem. Rev.*, 2003, **103**, 1979–2017.

58 H. C. Kolb, M. G. Finn and K. B. Sharpless, *Angew. Chem., Int. Ed.*, 2001, **40**, 2004–2021.

59 H. Zheng, B. Xu and T. M. Swager, *Chem. Mater.*, 1996, **8**, 907–911.

60 M. Lehmann, R. I. Gearba, M. H. J. Koch and D. A. Ivanov, *Chem. Mater.*, 2004, **16**, 374–376.

61 J. Barberá, L. Puig, J. L. Serrano and T. Sierra, *Chem. Mater.*, 2004, **16**, 3308–3317.

62 J. Barberá, M. Bardají, J. Jiménez, A. Laguna, M. P. Martínez, L. Oriol, J. L. Serrano and I. Zaragozano, *J. Am. Chem. Soc.*, 2005, **127**, 8994–9002.

63 E. Cavero, S. Uriel, P. Romero, J. L. Serrano and R. Giménez, *J. Am. Chem. Soc.*, 2007, **129**, 11608–11618.

64 The relationship between the density (ρ) of the compounds in the mesophase and the number of molecules per unit cell (Z) is given by the equation: $\rho = (M/N)/(V/Z)$, where M is the molar mass of the pure compound, N the Avogadro number, and V the unit cell volume (cm^3). In the case of a hexagonal symmetry of the cell unit, the volume is calculated by the formula $V = (\sqrt{3}/2)a^2c \times 10^{-24}$ where (a) and (c) are the lattice constants in Å.

65 E. Beltrán, E. Cavero, J. Barberá, J. L. Serrano, A. Elduque and R. Giménez, *Chem.–Eur. J.*, 2009, **15**, 9017–9023.

66 C. Reichardt, *Chem. Rev.*, 1994, **94**, 2319–2358.

67 I. A. Levitsky, K. Kishikawa, S. H. Eichhorn and T. M. Swager, *J. Am. Chem. Soc.*, 2000, **122**, 2474–2479.

68 R. Fink, C. Frenz, M. Telakkat and H. W. Schmidt, *Macromolecules*, 1997, **30**, 8177–8181.

69 M. Mardelli and J. Olmsted, *J. Photochem.*, 1977, **7**, 277–285.

70 D. F. Eaton, *Pure Appl. Chem.*, 1988, **60**, 1107–1114.